

Guiding the exploration of the solution space in walking robots through growth-based morphological development

Martín Naya-Varela[†]

Integrated Group for Engineering
Research and CITIC, Universidade
da Coruña, Spain
martin.naya@udc.com

Andrés Faiña

Computer Science Department and
REAL Lab, IT University of
Copenhagen, Denmark
anf@itu.dk

Richard J. Duro

Integrated Group for Engineering
Research and CITIC, Universidade
da Coruña, Spain
richard@udc.es

ABSTRACT

In human beings, the joint development of the body and cognitive system has been shown to facilitate the acquisition of new skills and abilities. In the literature, these natural principles have been applied to robotics with mixed results and different authors have suggested several hypotheses to explain them. One of the most popular hypotheses states that morphological development improves learning by increasing exploration of the solution space, avoiding stagnation in local optima. In this article, we are going to study the influence of growth-based morphological development and its nuances as a tool to improve the exploration of the solution space. We will perform a series of experiments over two different robot morphologies which learn to walk. Furthermore, we will compare these results to another optimization strategy that has been shown to be useful to favor exploration in learning algorithms: the application of noise during learning. Finally, to check if the increased exploration hypothesis holds, we visualize the genotypic space during learning considering the different optimization strategies by using the Search Trajectory Network representation. The results indicate that noise and growth increase exploration, but only growth guides the search towards good solutions.

CCS CONCEPTS

• **Computing methodologies** → **Machine learning** → **Machine learning approaches** → **Bio-inspired approaches**;

KEYWORDS

Developmental Robotics, Legged Robots, Search Trajectory Network, Noise.

ACM Reference format:

Martin Naya-Varela, Andrés Faiña and Richard J. Duro. 2023. Guiding the exploration of the solution space in walking robots through growth-based morphological development. In *Proceedings of the Genetic and Evolutionary Computation Conference 2023 (GECCO '23)*. ACM, New York, NY, USA, 9 pages. <https://doi.org/10.1145/3583131.3590489>

Permission to make digital or hard copies of part or all of this work for personal or classroom use is granted without fee provided that copies are not made or distributed for profit or commercial advantage and that copies bear this notice and the full citation on the first page. Copyrights for third-party components of this work must be honored. For all other uses, contact the owner/author(s).

GECCO '23, July 15-19, 2023, Lisbon, Portugal
© 2023 Copyright is held by the owner/author(s).
ACM ISBN 979-8-4007-0119-1/23/07...\$15.00
<https://doi.org/10.1145/3583131.3590489>

1 INTRODUCTION

In humans and animals, morphological development from infancy to adulthood has been shown to facilitate learning [1], [2]. To improve the learning performance of different robotic morphologies, some of the developmental principles observed in nature have been tested in different robots and scenarios. The application of these morphological development principles to robotics has led to mixed results being, depending on the case, helpful [3]–[5], irrelevant [6], [7], or even detrimental [8], [9] for learning.

It is not easy to extract a clear notion of the effects of morphological development on the learning abilities of robots and why they are influenced by such morphological change. Nevertheless, some authors have provided some indications based on the conclusions provided by the results of their experiments.

For example, using a three-finger hand learning to grasp different geometric objects, Bongard [7] related the influence of morphological change when learning to task complexity. When the hand had to grasp two or three different kinds of object morphologies, the learning performances of morphological development increased compared to the no-development case. Similar conclusions were extracted from Bongard and Buckingham [10] in a four-wheeled robot in two simulators with different levels of fidelity with respect to reality. Another factor that is claimed to influence learning are abrupt changes in morphology. In an experiment with quadruped and hexapod robots that learn to walk, Bongard [11] hypothesizes that an abrupt change in the controller-morphology relationship decreases the performance because the learning algorithm needs time to adapt the controller to the new morphology. Similar conclusions were reported by Lungarella and Berthouze [12] in a bipedal mechanism that was learning to swing under an external perturbation. The morphological development mechanism that implied freezing and freeing Degrees of Freedom (DOF) led to instabilities in the system, making it harder to find adequate robotic swinging behavior. Finally, in a bipedal walking example, Zhu et al. [13] observed how morphological development has helped to learn to walk thanks to the initial stability that a tripod configuration confers to the body and the early stages of learning. Such an increase in stability was also mentioned as a relevant factor by Naya-Varela et al. both in a quadruped [14] and bipedal morphology [15].

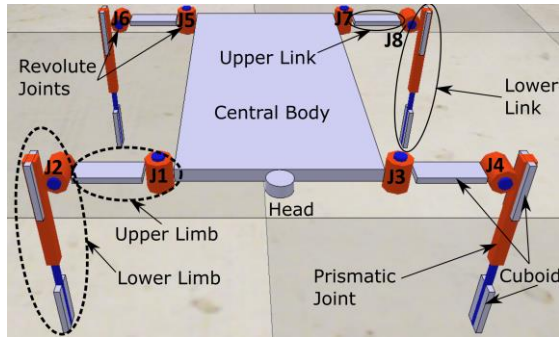


Figure 1. Quadruped with 8 DOF and detail of the different parts of the morphology with the name of the joints.

In the literature, one of the most predominant hypotheses about why learning in morphological development-based experiments outperforms the no-development ones is attributed to the fact that morphological development favors the exploration of the solution space, avoiding stagnation in local optima. This was suggested by Lungarella and Berthouze [12] and also by Naya-Varela et al. [16] who reported similar conclusions in a growth-based morphological development quadruped robot experiment. On the other hand, Benureau and Tani [17], consider that morphological wobbling helps to avoid getting trapped in local optima of the behavioral space, presenting some qualitative results that support their hypotheses.

In this article, we are going dig deeper into the implications of morphological development as a tool to improve learning. Concretely, we will analyze whether morphological development is just another optimization technique that helps to avoid stagnation thanks to increasing the random exploration of the solution space, or whether it presents some nuances that makes it different compared to other optimization techniques. Thus, in a group of experiments over two different morphologies, we will compare the results obtained selecting growth as a morphological development strategy during learning to the learning results with no growth while noise is added during learning to the same morphologies. The application of noise was selected to compare with morphological development because it is a straightforward manner of introducing random exploration of the solution space that has already been used in the literature, with good results, to improve learning by avoiding stagnation in local optima [18]–[20], leading to more robust learning by favoring the adaptation of the algorithm to the environmental conditions [21]. Furthermore, the results and implications of both morphological development and noise will be compared and analyzed by means of their impact on a representation using Search Trajectory Networks (STN) [22] to provide the possibility of visual and quantitative analysis of the different learning trajectories followed by each type of experiment. A first approximation to the comparison between morphological development and noise was carried out by Naya-Varela et al. [23]. However, in that article, the authors only considered one type of morphology and noise implementation. They did not go into details about the implications of noise on the learning process and how it affects the evolution of the robot controllers.

Thus, here we have carried out a series of experiments over growth-based morphological development using two morphologies, a quadruped and a bipedal robot, several types of noise, including morphological noise, and visualized how they explore the search space.

2 EXPERIMENTAL SETUP

In the following, we describe the morphology of each robot that was considered in this study, as well as the different experiments carried out with them and their characteristics.

2.1 Morphology

The experimental framework was set up in simulation, and considered simplified morphological changes. In it, two different morphologies have been used, a quadruped and a modified version of the NAO robot [24] that allows the NAO to grow.

On the one hand, the quadruped morphology (Figure 1) is composed of a central body and four limbs attached to it. The limbs are constructed from an upper link and a lower link with their revolute joints. The upper link measures 5x2.5x0.5 cm and has a mass of 250 g, while the lower link is made up of two elements, with the same dimensions and mass as in the upper link, joined by a prismatic joint. This prismatic joint is the element of the morphology that allows the robot to grow. The prismatic joint can apply a maximum force of 50 N and it is controlled by a proportional controller ($P = 0.1$). All the prismatic joints of the legs have a maximum stroke of 7.5 cm, which means that the length of the lower link may vary from 10 cm (lower link fully contracted) to 17.5 cm (lower link fully extended). In addition, there are two revolute joints in each limb that join the central body and the upper link, and the upper link and the lower link, respectively. All the revolute joints are actuated and have a maximum Range of Motion (ROM) of $[-90^\circ, 90^\circ]$. Their maximum torque is 2.5 Nm and they are also controlled through a proportional controller ($P = 0.1$).

On the other hand, the morphology of the bipedal robot is based on the simulation model of the real NAO robot in the CoppeliaSim simulator [25]. However, several changes have been made to this simulation model, both to simplify the simulation model and to allow changes in the morphology of the robot while it develops:

Upper link: The upper part of the legs was changed from a single mesh to two cuboids, to allow for the growth of this part. Both cuboids have the same dimensions and weight, 8x8x7.2 cm. They are joined by a prismatic joint, which performs the extension of the upper part of the leg. It has a maximum force of 50 N. The maximum extension of the prismatic joint is 4.0 cm, which is almost a third of the size of the upper link when not extended. When fully contracted, the leg matches the original dimensions of the NAO. The mass of the upper link is $458 \text{ g} * 2 = 916 \text{ g}$.

Lower link: The lower part of the legs was also changed to two different cuboids. The upper cuboid presents a size of 8x3x8 cm with a mass of 192 g and the lower one has a size of 9x8x3 cm with a mass of 216 g. Again, the properties of the cuboids and their geometric orientation were selected to preserve the original NAO design. The prismatic joint presents the same functionality and

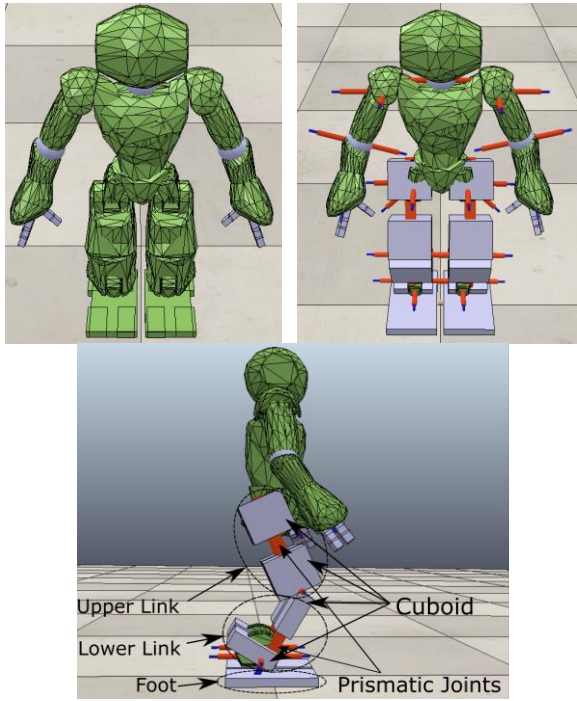


Figure 2. Top left: frontal view of the original NAO robot model in CoppeliaSim with the different meshes (*links*) of the model. Top right: frontal view of the developmental model of the NAO. In green, the default meshes of the original robot. In grey, the modified parts: the cuboids added to the robot to create the extendible upper and lower link and simplified feet. In red, the rotational and prismatic joints. Bottom: side view of the NAO model where its different parts are indicated.

properties as the one of the upper link: a maximum force of 50 N and a maximum extension of 4.0 cm.

Foot: The foot size and weight have also been modified with respect to the native design of the NAO robot of the CoppeliaSim. The simulation model was simplified, reducing the number of cuboids that constitute the original foot of the NAO. Now, each foot is 18.4x10x1.5 cm in size and weighs 276 g.

2.2 Controller

The controller of the robots is a Neural Network (NN) with a sigmoid activation function. Learning is achieved through a neuroevolutionary process using the NEAT algorithm [26], concretely, the MultiNEAT implementation [27]. The initial configuration of the NN is different for each morphology. For the quadruped, the NN has one input plus bias and 8 outputs, one for each joint of the robot. For the NAO, the NN has 3 inputs plus bias and 14 outputs. These outputs control the different movements of the NAOs legs as well as the shoulders. The weights and structure of the NN represent the genome of the learning algorithm. The inputs of the NN are only sinusoidal signals, as pattern generators, to simplify the study on the influence of morphological development and noise addition during learning, avoiding the cross influence that they may cause over the sensory system. For the

Table I. Values of the maximum ROM available for each joint of the bipedal robot in degrees.

Joint	ROM
Right and Left Shoulder Pitch	[-20.0, 50.0]
Right and Left Ankle Roll	[-30.0, 30.0]
Right and Left Ankle Pitch	[-65.0, -5.0]
Right and Left Knee Pitch	[25.0, 85.0]
Right and Left Hip Pitch	[-50.0, 10.0]
Right and Left Hip Roll	[-20.0, 20.0]
Right and Left Hip Yaw Pitch	[0.0, 0.0]

quadruped, the sinusoidal function has an amplitude of 2 and an angular velocity of 10 rad/s. For the NAO, the sinusoidal functions have an amplitude of 2 and a frequency of $2.21 * \pi$ rad/s, with phases 0, $\pi/3$, and $\pi/5$ rad respectively. The outputs of the NN are denormalized from the sigmoid output interval [0, 1] to the ROM available for each joint. In the case of the quadruped, this ROM is defined by the interval $[-90^\circ, 90^\circ]$, as already mentioned. In the case of the NAO, this denormalization also depends on the maximum ROM available for each joint, displayed in Table I.

2.3 Simulator and evolutionary setup

The experiments are performed in the CoppeliaSim simulator with the Open Dynamics Engine [28] as the physics engine. Every independent run of NEAT starts from an artificial neural network with a full connection between the input neurons and the output neurons and without any hidden layers. NEAT evolves a population of 50 individuals for 300 generations. To gather statistical data, 50 independent runs were carried out for each experiment. The fitness of an individual is calculated directly as the straight-line distance traveled by the head of the robot in the horizontal plane. Each individual of the population is tested for 3s in the case of the quadruped and 5 s in the case of the NAO, with a simulation time step of 50 ms and a physics engine time step of 5 ms. For the quadruped, the NN is updated every two simulation time steps (100 ms). For the NAO, the NN is updated each time step (50 ms). This difference is motivated by the morphological differences between both robots, which implies that the quadruped needs more time to perform the movement of the joints, leading to strange solutions when only one simulation time step is considered.

2.4 Experiments

Two different kinds of experiments have been performed over these two morphologies: the reference experiments and the gaussian noise ones.

No development experiment: A fixed morphology corresponding to the final morphology for the rest of the experiments (maximum length of the limbs) was used for the whole neuroevolutionary process in the case of each morphology.

Growth experiment: The robot morphology grows during the learning process starting from the shortest version of the links in generation 0 (fully contracted) until reaching the final morphology

(fully extended). For the quadruped, the fully contracted link length is 10 cm, while when fully extended it is 17.5 cm. In this case, link length is grown linearly and simultaneously for all the legs for 60 generations until it reaches the final morphology. After that, neuroevolution may continue, but without changes in the morphology. For the NAO, the upper link length when fully contracted is 14.4 cm, while when fully extended is 18.4 cm. The fully contracted lower link length is 11 cm, which when fully extended goes up to 15 cm. The links grow linearly until generation 150 when they reach the final morphology. The robots do not grow during the individual evaluations, that is, each growth step is applied before the beginning of each evaluation.

Noise experiments: Three types of noise experiments have been constructed to perform controlled perturbations to the system, in consonance with our experimental setup: (1) Noise addition at the input of the NN, (2) noise addition at the output of the NN, and (3) noise addition to the robot morphology, concretely to the size of the leg, over the same actuator that performs the growth of the morphology. These experiments are applied over the final and fixed morphology of each experiment. Noise is generated by a Gaussian Function (GF), with $\mu = 0$. Several σ values have been selected to adjust the noise level according to the position where it is added (input to the NN, output to the NN and in the leg extension of the final morphology for each one) and also to provide different noise levels according to the magnitude they perturb, having the possibility of even doubling its value. Table II summarizes the different σ for each case and experiment. Thus, noise is added in the following forms:

- Input to the NN (Input noise):
 $Input = 2.0 * \sin(\omega * t) + GF(0, \sigma_{input})$
- Output to the NN (Output noise):
 $Output = NN \text{ output} + GF(0, \sigma_{output})$
- In the morphology (morphological noise):
 $Leg \text{ extension} = Leg \text{ size} + GF(0, \sigma_{morphology})$

As the objective of these perturbations is to analyze the effects of noise over the learning process and compare it to the effects of growth-based morphological development, the noise was applied to the quadruped and NAO during the same number of generations as in the case of growth for each morphology. After that, learning continues without noise, similar to what happens in the growth experiment.

2.5 Search Trajectory Networks

Search Trajectory Networks (STN) is a graph-based tool to analyze and visualize the behavior of population-based algorithms. It describes the trajectory of the best solution over time. The visualizations and metrics of STNs provide an additional tool for analyzing algorithm behavior that may provide insights that are not captured by the traditional representation of the fitness value during

Table II. Sigma values for the perturbations generated at the input and output of the NN and in the morphology.

	Input	Output	Morphology
σ_1	1	0.3	0.01
σ_2	2	0.5	0.1
σ_3	3	1	0.2

the evolutionary process and the statistical analysis. We utilize STNs to study the trajectory described by the best solution obtained in each generation on 5 independent and randomly selected executions for each experiment, with the aim of evaluating the exploration ability of the learning algorithm in each of the experimental conditions and to relate it with the performance obtained. To that end, for each best solution we consider its fitness value and the genotype. The genotype includes the topology of the NN in the following form:

$$genotype = [sn_1, tn_1, wv_1 \dots sn_n, tn_n, wv_n]$$

Where:

- sn: means “source neuron” and it is the neuron from which the synapsis for that weight starts.
- tn: means “target neuron” and it is the neuron where the synapsis for that weight ends.
- wv: means “weight value” and it is the value of the weight that connects two neurons.
- And 1, 2, ..., n, is the number of weights in the NN.

In order to visualize the graphs, we used the Fruchterman-Reignold [29] implementation. In it, a node represents an area of the search space of similar genomes from a predefined partitioning of the search space. Edges represent interconnections among nodes. The size of the nodes is proportional to how many times a node is reached by the algorithm. More information about how the STNs are constructed can be found in the articles of the authors of this type of representation [22], [30].

3 RESULTS

In this section, we present the results of the learning process for each kind of experiment and the statistical analysis of the performance achieved at the end of learning, as well as the STN study for each morphology and experiment. The source code for the different experiments can be found in the repository¹.

3.1 Learning process

The top rows of Figures 3 and 4 represent in solid and dashed lines, the median of the best individual obtained in each independent execution for each type of experiment, being the growth experiment the blue one, and the black dashed lines represent the no development case. The red, orange, and green lines correspond to the different noise experiments, which are performed over the fixed and no development morphology. The shaded areas represent the interval between the 25 and 75 percentile. The bottom row displays the statistical results of the no development

¹ https://github.com/GII/morphological_development/tree/main/publications/2023_gecco

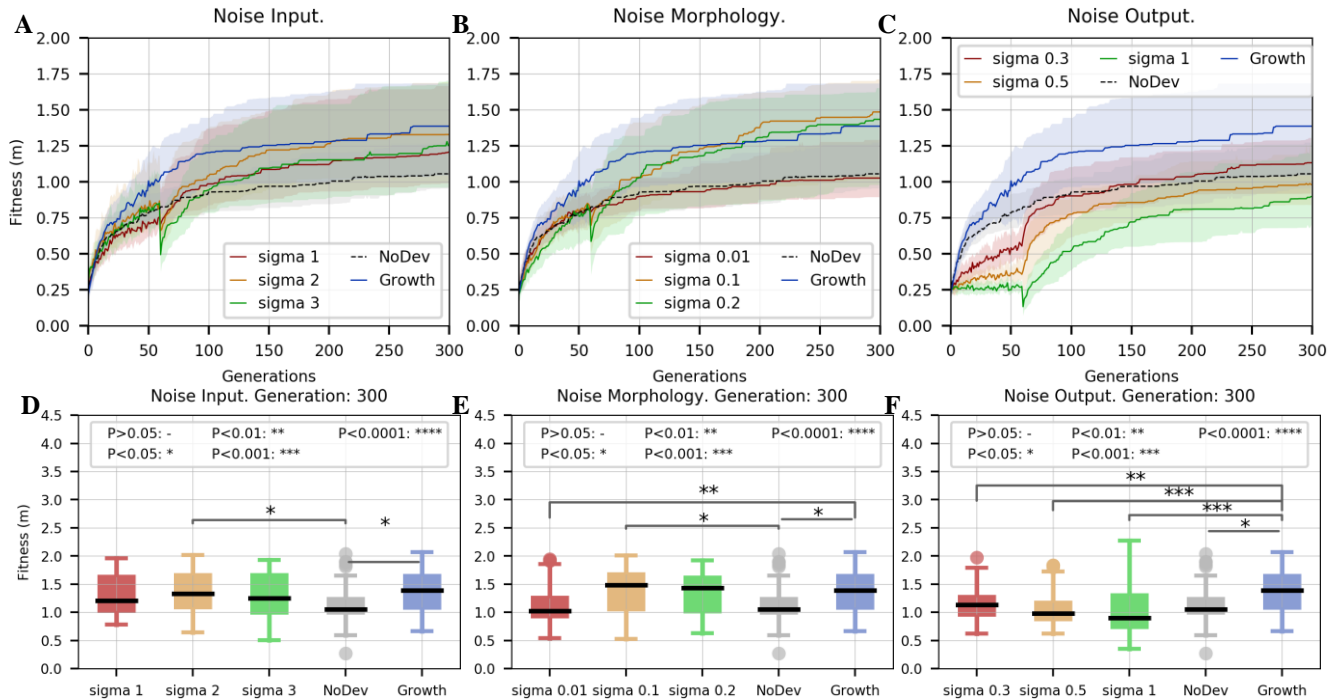


Figure 3. Quadruped morphology. Top: Results of the learning process during 300 generations for each experiment. Bottom: Statistical analysis at generation 300 comparing the growth experiment (blue) and the no development one (grey) with the other experiments. Left: Noise addition at the input of the NN. Middle: Noise addition to the leg size. Right: Noise addition at the output of the NN.

experiment and the growth one compared to the noisy experiments at the end of learning. Each boxplot corresponds to the median and the 75 and 25 quartiles. The whiskers are extended to 1.5 of the interquartile range (IQR). Single points are values that are out of the IQR. The statistical analysis has been carried out using the two-tailed Mann-Whitney U test [31]. We consider a p-value of 0.05 as the significant value for accepting or rejecting the null hypothesis (the compared samples are equal). The numerical values of the statistical analysis have been replaced by asterisks for simplicity. A Bonferroni correction [32] has been applied to the statistical analysis.

Regarding the quadruped morphology, we can first observe how growth-based morphological development has outperformed the no development case, achieving a p-value of 0.01 (Figure 3 bottom row) and during the learning period, the median of the growth experiment is always above the median of the no development experiment (Figure 3 top row). On the other hand, Figure 3A and Figure 3D show how the application of noise at the input of the NN has only improved learning with respect to the no development case in one instance ($\sigma=2$ with p-value of 0.0221), being irrelevant when compared to growth. The application of noise to the morphology has been shown to be favorable for learning in the case of $\sigma=0.1$, compared to the no development case (Figure 3E, p-value of 0.0117). On the other hand, noise with $\sigma=0.01$ has been shown to be detrimental for learning when compared to growth (p-value of 0.0048). Finally, the application of noise at the outputs of the NN has turned out to be irrelevant compared to the no development case (Figure 3F). On the other hand, it was clearly detrimental when

compared to growth, presenting p-values of 0.0085, 0.0001 and 0.0002. For this group of experiments, it can be observed how as the level of the perturbation increases, the performance of the noise experiments decreases, indicating that such strong perturbations in the controller-morphology relationship in morphological development negatively influence learning, as other authors have mentioned before [8], [9].

Regarding the NAO morphology, the growth experiment clearly outperforms the no development one, as displayed in the bottom row of Figure 4, achieving a p-value of $7 \cdot 10^{-5}$. The input noise (Figure 4J) and morphological noise (Figure 4K) experiments have been shown to be irrelevant for learning compared to the no development case. On the other hand, the application of noise at the output of the NN (Figure 4N) has been clearly detrimental, leading to the worst results, (p-values of $3 \cdot 10^{-5}$, 0.0003 and 0 for the $\sigma=0.3$, $\sigma=0.5$ and $\sigma=1$ experiments respectively) especially during the noise phase, where there is not any value different from 0. These results show how perturbations in the output of the NN, or at least such a level of perturbations, are not suitable exploratory techniques in this case. On the other hand, growth-based morphological development has been shown to improve the learning results of all the noise experiments, although with different levels of significance.

Once these results were obtained, we asked what would happen if we combined growth with noise, because in the previous cases, growth was performed without any perturbation of the system. To answer that, we selected the already deployed growth experiment for each morphology and combined it with the noise strategy that

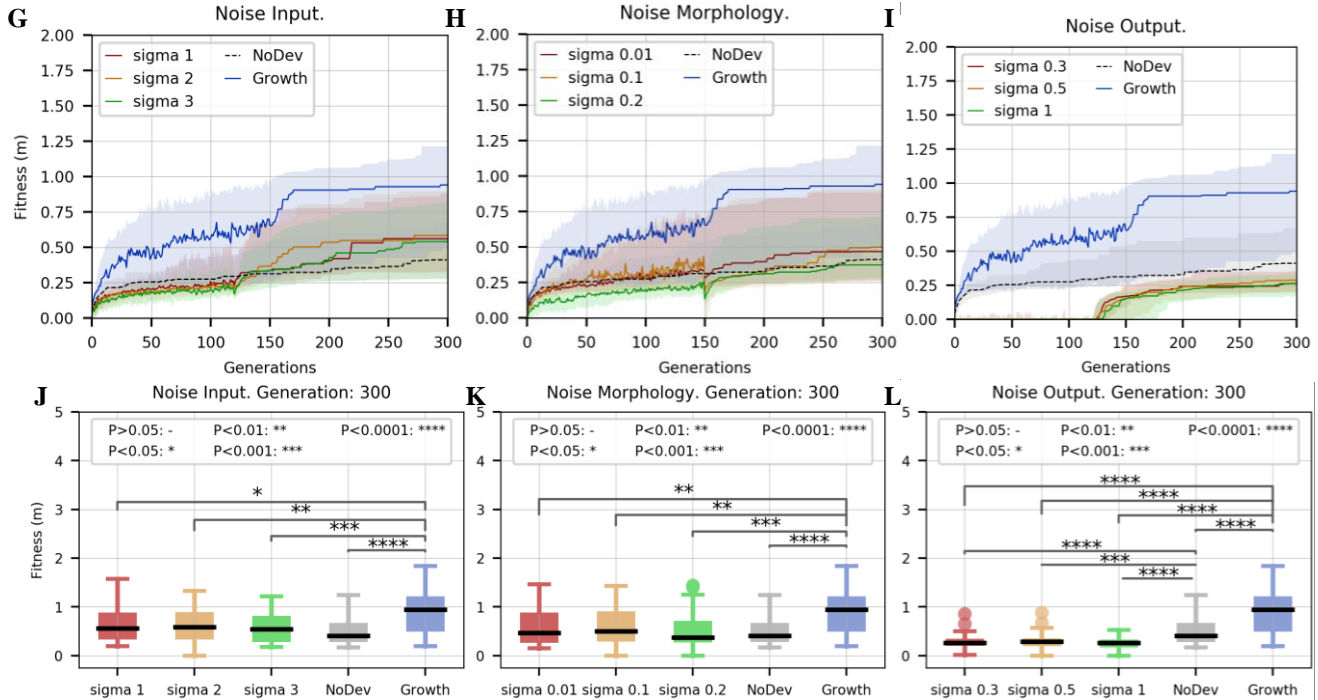


Figure 4. Bipedal morphology. Top: Results of the learning process during 300 generations for each experiment. Bottom: Statistical analysis at generation 300 comparing the growth experiment (blue) and the no development one (grey) to the other experiments. Left column: Noise addition at the input of the NN. Middle column: Noise addition in the leg size. Right column: Noise addition at the output of the NN.

gave the best results for each type of noise experiment in the quadruped morphology. We have selected the morphology of the quadruped as a reference because it is the one in which there are noise experiments that outperform the no development ones. Thus, the selected noise experiments are: $\sigma=2$ for the noise input experiment, $\sigma=0.1$ for the noisy morphology experiment, and $\sigma=0.3$ for the noise output experiment. Results (Figure 5) show how the combination of growth and noise did not outperform the experiment that considered only growth. Nevertheless, in the quadruped morphology, such a combination has yielded good results in the case of input noise and growth when compared to the no development experiment. In this case, a higher statistical difference is achieved instead of only growth (p-value of 10^{-5} for the combined experiment against 0.01 for only growth). For the NAO morphology, the combination of noise and growth has yielded mixed results. On the one hand, the combination of output noise and growth has been detrimental to learning, which seems to indicate that the addition of noise at the outputs of the NN is clearly

detrimental to learning in view of the results of Figure 4L and Figure 5P. On the other hand, the combination of growth and noise in the morphology has led to better results than applying only noise compared to the no development case. For the rest of the experiments, there is no improvement using the combination of both optimization strategies.

3.2 Search Trajectory Network representation

Figure 6 represents the STN representation of 5 independent executions for each experiment: growth, no development, and noise for each morphology and Table III displays the number of nodes and edges for each STN representation. From Figure 6 and Table III, we can observe how the same type of experiment shares similarities between morphologies. On the one hand, the experiment with the lowest number of nodes and edges for each morphology is the no-development experiment (Figure 6R and Figure 6U). On the other hand, the experiment with the highest

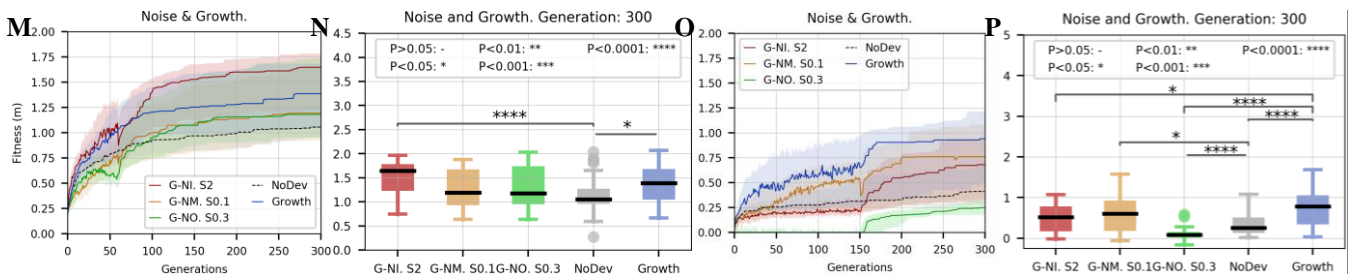


Figure 5. Results combining the growth-based morphological development with the noise ones. M and N figures: experiments with the quadruped morphology. O and P figures: experiments with the bipedal morphology.

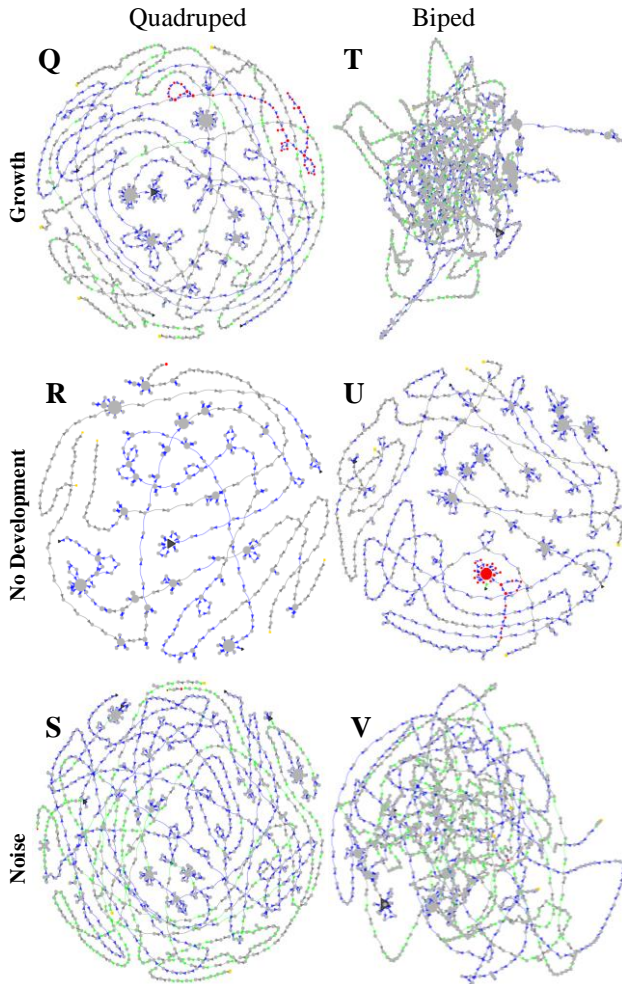


Figure 6. Search Trajectory Network representations using growth, no development and morphological noise experiments ($\sigma=1$) for 5 runs. Red dots indicate the best genomes for the group of experiments, the yellow ones, the starting genomes and the grey ones, intermediate genomes. Green arrows indicate a reduction of the fitness value between genomes, and blue arrows indicate that the fitness value is maintained between genomes.

number of nodes is the noise experiment (Figure 6S and Figure 6V), being the growth experiment the intermediate one (Figure 6Q and Figure 6T). Comparing the number of nodes of the growth and noise experiment against the no development one, we can observe how the number of nodes increases to 193% and 258% respectively for the quadruped, and 236% and 213% for the NAO. Furthermore, the STNs of Figure 6R, and Figure 6U show more than one node that represents the best solution. However, by paying attention to the figure, these different best nodes are connected by blue lines, meaning that the fitness value of the best solutions does not change. That is, in those experiments, the same fitness value can be achieved by different genomes. Finally, the no-development experiments of each morphology are characterized by displaying

only blue and grey lines, while the growth and the noise one also display green lines, indicating a reduction in the fitness value.

4 DISCUSSION

In the quadruped morphology, noise has been shown to be relevant for learning only when it is applied at the input of the neural network, and to the morphology (Figure 3A and Figure 3B). For the NAO morphology, noise has not been shown to be favorable compared to no development, and only relevant when it was combined with growth (Figure 5P).

These differences among the noise, the no development, and the growth experiments can be explained using the different STN representations. The STNs of the no-development experiments for each morphology display the lowest number of nodes and edges. That is, for the same number of generations the no developmental experiments result in the lowest degree of disparity in the solutions found, i.e. least exploration. The NAO experiment displays a higher disparity than the quadruped motivated by two reasons: 1) STNs are highly influenced by the number of weights of each NN: we have 16 weights at the beginning of learning for the quadruped and 56 for NAO, which facilitates the emergence of different genomes during the neuroevolutionary process. 2) The “needle in the haystack problem” [33] that finding solutions in the NAO problem seems to represent, often leads to a higher exploration of the search space, due to the lack of good guides to exploit. Such a low level of disparity in the population can be related to the learning stagnation displayed in Figure 3 and Figure 4.

For the quadruped the highest number of nodes and edges are found in the noise experiment. For the NAO, it was found for the growth experiment. This means that the solutions found of these experiments display the highest level of disparity during learning, i.e. highest level of exploration. Such a level of disparity is well represented in Figure 6T and Figure 6V, in which the program that automatically performs the STN representation is not able to manage such a number of nodes and edges as easily as it manages them for the other experiments. This level of disparity is motivated by the continuous change of the morphology that noise and growth produce, meaning an increment or decrement of the fitness values, something that does not happen in the case of no development, where the fitness value is always improved or preserved (as there is elitism in the evolutionary algorithm). This level of disparity can be comparable to an increase in the exploratory behavior of the learning algorithm to avoid stagnation in local optima.

Thus, although growth and noise experiments display a high level of exploration of the solution space, it seems that the relevance of the growth-based experiments cannot be only attributable to the fact that it increases the exploratory behavior, otherwise, we would presume that both learning strategies should present similar results. Then, there must be other causes that make morphological development improve learning. These causes can be explained by observing the differences between learning with the NAO and the quadruped. These differences are motivated by the complexity of learning to walk with each morphology. As mentioned, learning to walk with the NAO is much more difficult

Table III. Number of nodes and edges obtained for each kind of experiment for the 5 independent executions. The no development experiment has been abbreviated by “No dev.”

		Nodes	Edges
Quadruped	No dev.	333	421
	Growth	643	749
	Noise	858	964
NAO	No dev.	502	632
	Growth	1187	1253
	Noise	1067	1141

than learning with the quadruped. Due to its morphological configuration, the quadruped presents an intrinsic stability that the NAO does not display. Such higher stability allows the quadruped to be more tolerant to system perturbations. These perturbations may decrease the efficiency of the gaits obtained, reducing the fitness values, but it is harder to find perturbations that cause dramatic falls leading to the impossibility of continuing walking. However, in the NAO, small perturbations can cause the failure of the walking behavior, ending up with the NAO sprawled on the ground. Hence, the NAO requires a more precise controller to displace that permits always preserving its upright position, something that seems to be very challenging in view of the results.

As a consequence, the application of noise to the robot controller or morphology, which implies random perturbations, does not lead to the effect that growth based morphological development produces. Growth implies a controlled development of the morphology from an initial and more stable morphology, that presumably simplifies learning at the beginning, to the final and more unstable one. This simplification of learning at the beginning is translated into a modification of the solution space, allowing a greater number of valid and informative solutions than can be obtained when considering the final morphology. During the developmental phase, the robot morphology gradually changes, smoothly modifying the characteristics of the solution space, progressively reducing the number of solutions available. Such gradual modification of the solution space sets a “developmental path” that guides the optimal solution throughout the different developmental stages, from easier stages to more complex ones. That is, at the beginning, morphological development helps to widen the attractor basin of the optimal solutions, facilitating the task of the learning algorithm to find it. As development takes place, the attractor basin is gradually reduced, and the developmental process itself pushes the learning algorithm toward the optimum of each developmental stage, until reaching the optimum in the final one, setting the “developmental path”. Furthermore, during development the solution space is constantly changing, helping to prevent learning stagnation. Such guidance does not happen when just adding noise. Due to the gaussian noise selected, exploration is increased around the parameters that define the genotype of the individual in the solution space, but it suffers from the lack of the “developmental path” set by growth and its gradual modifications of the solution space, hypothesis supported by the work of Naya-Varela et al. [15]. Hence, the developmental process is less relevant in the case of the quadruped due to its intrinsically more stable morphology, simplifying the task of finding optimal solutions in

the solution space, but it is determinant in the NAO due to the difficulty of finding the attractor basing of optimal solutions in the “needle in a haystack” problem we have.

Furthermore, we consider that learning strategies based on the variation of the morphology such as morphological wobbling [17] or adaptive morphology [34] should not be considered morphological development strategies. We argue that those strategies suffer from the lack of guide that the learning algorithm has in a morphological development process, with all the nuances that it involves. Hence, those optimization strategies which also reported good results would be closer to the characteristics of our noise experiments, in terms of increasing exploration and avoiding stagnation.

5 CONCLUSIONS

Throughout this article, we have studied the implications of growth-based morphological development as a strategy to improve learning by means of analyzing its exploration ability and guidance of the learning algorithm. We have found how different results are obtained for a quadruped and a NAO biped morphology. Such disparity is related to the difficulty of the problem each morphology has to face and with the characteristics of their solution spaces. Learning to walk with the quadruped is easier than learning to walk with the biped, which implies that optimal solutions in the solution space are harder to find for the latter. In this context, the quadruped is more amenable to perturbations that may lead to finding areas in the solution space that improve the performance of standard learning. However, due to the higher complexity of learning to walk with the NAO, the system is more rigid to external perturbations, which have not led to any improvement over the standard learning experiment. Only growth development and also its combination with noise have led to good results, motivated by the induced stability of the growth process and the simplification of the solution space that it obtains for the initial morphologies. Furthermore, the exploration ability of both strategies has been displayed in the STN representation. It was shown how, although both strategies have led to increasing the exploration of the solution space compared to the reference experiment, increasing only exploration and avoiding stagnation is not enough to improve performance. Other nuances, related to choosing an appropriate path from a simpler and more stable morphology, allowing a precise exploration of gaits, to the final one, as provided by growth in this case, are required.

ACKNOWLEDGMENTS

Research supported by the European Commission Horizon program PILLAR-Robots project, grant 101070381, the Xunta de Galicia and the European Regional Development Funds under grant EDC431C-2021/39, the Spanish Science and Education Ministry through grant PID2021-126220OB-100. M. Naya-Varela wish to acknowledge the support received by the Xunta de Galicia with his grant ED481B. We wish to acknowledge the support received from the Centro de Investigación "CITIC", funded by Xunta de Galicia and the European Union (European Regional Development Fund-Galicia 2014-2020 Program), by grant ED431G 2019/01 and the Centro de Supercomputación de Galicia (CESGA).

REFERENCES

- [1] E. Thelen, «Motor development as foundation and future of developmental psychology», *International Journal of Behavioral Development*, vol. 24, n.º 4, pp. 385-397, 2000, doi: 10.1080/016502500750037937.
- [2] J. Piaget y M. Cook, *The origins of intelligence in children*, vol. 8, n.º 5. International Universities Press New York, 1952.
- [3] A. Baranes y P.-Y. Oudeyer, «Maturationally-constrained competence-based intrinsically motivated learning», en *IEEE 9th International Conference on Development and Learning*, IEEE, 2010, pp. 197-203.
- [4] F. Chao, M. H. Lee, y J. J. Lee, «A developmental algorithm for ocular-motor coordination», *Robotics and Autonomous Systems*, vol. 58, n.º 3, pp. 239-248, 2010, doi: 10.1016/j.robot.2009.08.002.
- [5] S. Kriegman, N. Cheney, F. Corucci, y J. Bongard, «A minimal developmental model can increase evolvability in soft robots», en *Proceedings of the Genetic and Evolutionary Computation Conference*, ACM, 2017, pp. 131-138.
- [6] P. Savastano y S. Nolfi, «Incremental learning in a 14 DOF simulated iCub robot: Modeling infant reach/grasp development», *Lecture Notes in Computer Science (including subseries Lecture Notes in Artificial Intelligence and Lecture Notes in Bioinformatics)*, vol. 7375 LNAI, pp. 250-261, 2012, doi: 10.1007/978-3-642-31525-1_22.
- [7] J. Bongard, «The utility of evolving simulated robot morphology increases with task complexity for object manipulation», *Artificial Life*, vol. 16, n.º 3, pp. 201-223, 2010, doi: 10.1162/artl.2010.Bongard.024.
- [8] L. Berthouze y M. Lungarella, «Motor skill acquisition under environmental perturbations: On the necessity of alternate freeing and freeing of degrees of freedom», *Adaptive Behavior*, vol. 12, n.º 1, pp. 47-64, 2004, doi: 10.1177/105971230401200104.
- [9] V. Ivanchenko y R. A. Jacobs, «A developmental approach aids motor learning», *Neural Computation*, vol. 15, n.º 9, pp. 2051-2065, 2003, doi: 10.1162/089976603322297287.
- [10] D. Buckingham y J. Bongard, «Physical scaffolding accelerates the evolution of robot behavior», *Artificial Life*, vol. 23, n.º 3, pp. 351-373, 2017.
- [11] J. Bongard, «Morphological change in machines accelerates the evolution of robust behavior», *Proceedings of the National Academy of Sciences*, vol. 108, n.º 4, pp. 1234-1239, 2011, doi: 10.1073/pnas.1015390108.
- [12] M. Lungarella y L. Berthouze, «Adaptivity via alternate freeing and freeing of degrees of freedom», *ICONIP 2002 - Proceedings of the 9th International Conference on Neural Information Processing: Computational Intelligence for the E-Age*, vol. 1, pp. 482-487, 2002, doi: 10.1109/ICONIP.2002.1202217.
- [13] J. Zhu, C. Rong, F. Iida, y A. Rosendo, «Bootstrapping Virtual Bipedal Walkers with Robotics Scaffolded Learning», *Frontiers in Robotics and AI*, vol. 8, 2021, doi: 10.3389/frobt.2021.702599.
- [14] M. Naya-Varela, A. Faina, A. Mallo, y R. J. Duro, «A study of growth based morphological development in neural network controlled walkers», *Neurocomputing*, vol. 500, pp. 279-294, 2022, doi: <https://doi.org/10.1016/j.neucom.2021.09.082>.
- [15] M. Naya-Varela, A. Faina, y R. J. Duro, «Engineering morphological development in a robotic bipedal walking problem: An empirical study», *Neurocomputing*, vol. 527, pp. 83-99, 2023, doi: <https://doi.org/10.1016/j.neucom.2023.01.003>.
- [16] M. Naya-Varela, A. Faina, y R. J. Duro, «An Experiment in Morphological Development for Learning ANN Based Controllers», en *2020 International Joint Conference on Neural Networks (IJCNN)*, 2020, pp. 1-8. doi: 10.1109/IJCNN48605.2020.9206749.
- [17] F. C. Y. Benureau y J. Tani, «Morphological Wobbling Can Help Robots Learn», en *2022 IEEE International Conference on Development and Learning (ICDL)*, 2022, pp. 257-264. doi: 10.1109/ICDL53763.2022.9962194.
- [18] K. C. Tan, T. H. Lee, y E. F. Khor, «Evolutionary algorithms with dynamic population size and local exploration for multiobjective optimization», *IEEE Transactions on Evolutionary Computation*, vol. 5, n.º 6, pp. 565-588, 2001, doi: 10.1109/4235.974840.
- [19] M. Fortunato *et al.*, «Noisy Networks For Exploration», en *International Conference on Learning Representations*, 2018. [En línea]. Disponible en: <https://openreview.net/forum?id=rywHCPkAW>
- [20] J. Goldberger y E. Ben-Reuven, «Training deep neural-networks using a noise adaptation layer», en *International Conference on Learning Representations*, 2017. [En línea]. Disponible en: <https://openreview.net/forum?id=H12GRgcxg>
- [21] N. Jakobi, P. Husbands, y I. Harvey, «Noise and the reality gap: The use of simulation in evolutionary robotics», en *Advances in Artificial Life*, F. Morán, A. Moreno, J. J. Merelo, y P. Chacón, Eds., Berlin, Heidelberg: Springer Berlin Heidelberg, 1995, pp. 704-720.
- [22] G. Ochoa, K. M. Malan, y C. Blum, «Search trajectory networks: A tool for analysing and visualising the behaviour of metaheuristics», *Applied Soft Computing*, vol. 109, p. 107492, 2021, doi: <https://doi.org/10.1016/j.asoc.2021.107492>.
- [23] M. Naya-Varela, A. Faiña, y R. J. Duro, «Growth-Based Morphological Development: A Natural Approach to Fitness Landscape Shaping», en *Proceedings of the Genetic and Evolutionary Computation Conference Companion*, en GECCO '22. New York, NY, USA: Association for Computing Machinery, 2022, pp. 140-143. doi: 10.1145/3520304.3529049.
- [24] S. Shamsuddin *et al.*, «NAO», en *2011 IEEE International Conference on Control System, Computing and Engineering*, IEEE, 2011, pp. 511-516.
- [25] C. Robotics, «CoppeliaSim». 2022. Accedido: 4 de octubre de 2022. [En línea]. Disponible en: <https://www.coppeliarobotics.com/>
- [26] K. O. Stanley y R. Miikkulainen, «Evolving neural networks through augmenting topologies», *Evolutionary computation*, vol. 10, n.º 2, pp. 99-127, 2002.
- [27] P. Chervenski y S. Ryan, «MultiNEAT, project website», URL <https://www.multineat.com/>, 2012.
- [28] R. L. Smith, «Open Dynamics Engine». <https://www.ode.org/> (accedido 4 de octubre de 2022).
- [29] T. M. J. Fruchterman y E. M. Reingold, «Graph drawing by force-directed placements», *Software: Practice and Experience*, vol. 21, n.º 11, pp. 1129-1164, 1991, doi: <https://doi.org/10.1002/spe.4380211102>.
- [30] G. Ochoa, K. M. Malan, y C. Blum, «Search Trajectory Networks of Population-Based Algorithms in Continuous Spaces», en *Applications of Evolutionary Computation*, P. A. Castillo, J. L. Jiménez Laredo, y F. Fernández de Vega, Eds., Cham: Springer International Publishing, 2020, pp. 70-85.
- [31] P. E. McKnight y J. Najab, «Mann-Whitney U Test», *The Corsini encyclopedia of psychology*, p. 1, 2010.
- [32] H. Abdi, «Holm's sequential Bonferroni procedure», *Encyclopedia of research design*, vol. 1, n.º 8, pp. 1-8, 2010.
- [33] M. Naya-Varela, A. Faina, y R. J. Duro, «Harnessing Growth-Based Morphological Development to Facilitate Learning ANN-Controlled Bipedal Walking», en *2022 International Joint Conference on Neural Networks (IJCNN)*, 2022, pp. 1-8. doi: 10.1109/IJCNN55064.2022.9892609.
- [34] M. Garrad, J. Rossiter, y H. Hauser, «Shaping Behavior With Adaptive Morphology», *IEEE Robotics and Automation Letters*, vol. 3, n.º 3, pp. 2056-2062, 2018, doi: 10.1109/LRA.2018.2807591.